Double-strand DNA cleavage by copper complexes of 2,2′-dipyridyl with guanidinium/ammonium pendants†

Juan He,[a] Ping Hu,[a] Yu-Jia Wang,[a] Ming-Liang Tong,[a] Hongzhe Sun,[b] Zong-Wan Mao*[a] and Liang-Nian Ji[a]

Received 28th January 2008, Accepted 4th April 2008
First published as an Advance Article on the web 7th May 2008
DOI: 10.1039/b801549j

Two ligands with guanidinium/ammonium groups were synthesized and their copper complexes, $[Cu(L^1)Cl_2](ClO_4)_2\cdot H_2O$ (**1**) and $[Cu(L^2)Cl_2](ClO_4)_2$ (**2**) (L^1 = 5,5′-di[1-(guanidyl)methyl]-2,2′-bipyridyl cation and L^2 = 5,5′-di[1-(amino)methyl]-2,2′-bipyridyl cation), were prepared to serve as nuclease mimics. X-Ray analysis revealed that Cu(II) ion in **1** has a planar square CuN_2Cl_2-configuration. The shortest distance between the nitrogen of guanidinium and copper atoms is 6.5408(5) Å, which is coincident with that of adjacent phosphodiesters in DNA (*ca.* 6 Å). In the absence of reducing agent, supercoiled plasmid DNA cleavage by the complexes were performed and their hydrolytic mechanisms were demonstrated with radical scavengers and T4 ligase. The pseudo-Michaelis–Menten kinetic parameters (k_{cat}, K_M) were calculated to be 4.42 h^{-1}, 7.46 × 10^{-5} M for **1**, and 4.21 h^{-1}, 1.07 × 10^{-4} M for **2**, respectively. The result shows that their cleavage efficiency is about 10-fold higher than the simple analogue $[Cu(bipy)Cl_2]$ (**3**) (0.50 h^{-1}, 3.5 × 10^{-4} M). The pH dependence of DNA cleavage by **1** and its hydroxide species in solution indicates that mononuclear $[Cu(L^1)(OH)(H_2O)]^{3+}$ ion is the active species. Highly effective DNA cleavage ability of **1** is attributed to the effective cooperation of the metal moiety and two guanidinium pendants with the phosphodiester backbone of nucleic acid.

Introduction

Transition metal complexes that cleave DNA under physiological condition are of current interest in the development of artificial nucleases.[1–11] One of approaches is to construct multi-functional models promoting phosphodiester hydrolysis through cooperation of metal ions and functional groups.[12–17] Of functional groups, the guanidinium group is one of the most representative. It contains two amines and an iminium in a plane forming a Y shape to establish its great stability as an ion in aqueous environment. Guanidinium, or protonated guanidine, has six potential hydrogen bond donors available, making it highly soluble in aqueous systems. These structural features make it an extremely advantageous functional group for the binding of carboxylates or phosphates in enzymes and antibodies *via* forming strong ion-pairs, which play a key role in many biological activities, such as molecular recognition and catalysis.[18–24] In peptides, guanidine, a residue of arginine, exists in the protonated form as a guanidinium ion, which functions as an efficient recognition moiety of anionic functionalities, such as carboxylate, phosphate and nitrate, through hydrogen-bonding.[25] The replacement of the amino groups of ethidium with guanidinium groups resulted in a marked gain of both affinity and sequence selectivity in recognition of AT binding sites in DNA.[26] In alkaline phosphatase and purple acid phosphatase,[27,28] the highly efficient cooperativity of a metal ion and Arg-guanidinium residues promoted phosphate monoester hydrolysis. In addition to their biological roles, guanidine derivatives are widely utilized in synthetic organic chemistry as strong bases. Indeed, chiral guanidine catalysts are attractive targets in organocatalysis.[29] However, few metal complexes with guanidinium groups used for DNA cleavage have been reported.[30]

We previously reported a few dipyridyl derivatives with tetraalkylammonium pendants and their Cu(II) complexes, such as $[Cu(L)_2Br](ClO_4)_5$, where L is 5, 5′-di[1-(triethylammonio)methyl]-2,2′-dipyridyl, as nuclease mimics.[31] We found that the Cu(II) complex exhibits strong affinity towards DNA binding by electrostatic interaction and high nuclease activity. Relative to a tetraalkylammonium ion, a guanidinium or ammonium ion has not only electrostatic interaction but also hydrogen-bonding to the phosphodiester backbone of nucleic acid. In view of these unique characteristics of the guanidinium group, we recently focused our efforts on the construction of complexes containing appended ammonium or guanidinium functionalities on the dipyridyl ligand to explore more fully the combination and cleavage of DNA (Scheme 1). We report herein their synthesis, structure, species distribution in solution, DNA affinity and nuclease activity.

[a]*MOE Key Laboratory of Bioinorganic and Synthetic Chemistry, School of Chemistry and Chemical Engineering, Sun Yat-Sen University, Guangzhou, 510275, China. E-mail: cesmzw@mail.sysu.edu.cn; Fax: +86 20 8411 2245; Tel: +86 20 8411 3788*

[b]*Department of Chemistry, the University of Hong Kong, Pokfulam Road, Hong Kong, China*

† Electronic supplementary information (ESI) available: ^{1}H NMR spectrum of L^1. ESI-MS spectrum of L^1. X-Ray crystal structure of **1** in which each perchlorate anion binds with the copper ion and the guanidinium group by weak coordination and hydrogen-bonding to form a network structure. T_m curves of complexes **1**, **2**, **3**. Agarose gel electrophoresis and corresponding time course plots showing cleavage of pBR322 DNA by complexes **1** and **2**. Agarose gel showing the influence of catalase for the cleavage ability of complexes **1** and **2**. Kinetics for the cleavage of plasmid pBR322 DNA by **3**. Agarose gel showing cleavage of 38 μM pBR322 DNA incubated with 150 μM of **1** in 20 mM buffer of different pH. CCDC reference number 632380. For ESI and crystallographic data in CIF or other electronic format see DOI: 10.1039/b801549j

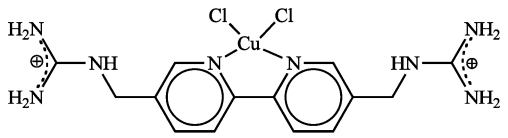

1

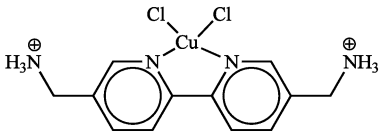

2

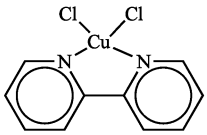

3

Scheme 1 Schematic illustration of complexes **1–3**.

Results and discussion

Molecular structure of 1

A prospective view of the cationic structure of **1** is shown in Fig. 1. along with selected bond distances and angles. The geometry around the copper(II) ion is square-planar with the basal plane formed by the two nitrogen atoms of the ligand and two chloride atoms [Cu(1)–N(1) and Cu(1)–Cl(1) distances are 2.024(3) and 2.2469(11) Å, respectively]. Since the guanidinium plane defined by N(2), N(3), N(4) and C(7) atoms adopts an extended conformation in the crystal stacking, the distance between Cu(1) and N(2) atoms is 6.5408(5) Å, which is coincident with that of adjacent phosphodiesters in B-form DNA (*ca.* 6 Å). Each perchlorate anion binds with the copper ion and the guanidinium group by weak coordination and hydrogen-bonding to form a network structure.

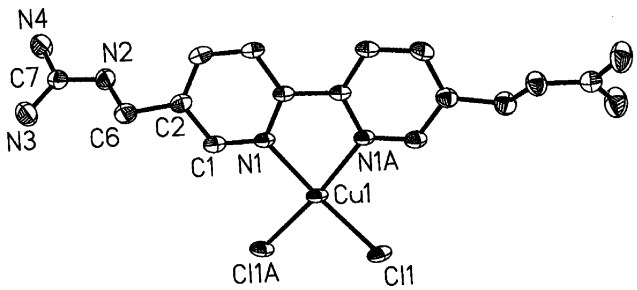

Fig. 1 Molecular structure of complex **1** with H atoms omitted for clarity; the other half of the complex is generated by the two-fold diad present in the space group *C*2/*c*. Key bond lengths (Å) and angles (°): Cu(1)–N(1) 2.024(3), Cu(1)–Cl(1) 2.2469(11), C(7)–N(2) 1.324(5), C(7)–N(3) 1.304(6), C(7)–N(4) 1.319(6); N(1)–Cu(1)–N(1A) 80.56(17), N(1)–Cu(1)–Cl(1A) 93.85(9), N(1)–Cu(1)–Cl(1) 171.05(9), Cl(1A)1–Cu(1)–Cl(1) 92.51(6), N(4)–C(7)–N(3) 119.4(4), N(2)–C(7)–N(3) 120.7(4), N(4)–C(7)–N(2) 119.9(41).

Species distribution of 1

The protonation constants (pK_n) of the ligands and their complex formation constants (K_{ML}) and the deprotonation constant (pK_a) of the coordinated water molecule as well as species distribution in solution were determined by potentiometric pH titration at 25 ± 0.1 °C. The pH profiles of the titration curves were analyzed and the calculated results were summarized (Table 1), including the distribution curves of the Cu(II) species as a function of pH (Fig. 2). Since the addition of NaCl did not cause any spectral changes (Fig. S9, ESI†), one can assume that the remaining coordination sites of Cu(II) are occupied by 2–4 water molecules.

Table 1 Species distribution and equilibrium constants of L^1 in the presence of Cu(II) ions

Reaction equilibrium	Constant	
$HL^{3+} = L^{2+} + H^+$	pK_a	2.19 ± 0.05
$[Cu(H_2O)_6]^{2+} + L^{2+} = [CuL(H_2O)_2]^{4+} + 4\,H_2O$	$\log K_{ML}$	4.23 ± 0.04
$2\,[CuL(OH)(H_2O)]^{3+} = [Cu_2L_2(OH)_2(H_2O)_2]^{6+}$	$\log K_{M_2L_2}$	5.81 ± 0.34
$[CuL(H_2O)_2]^{4+} = [CuL(OH)(H_2O)]^{3+} + H^+$	$pK_{a(ML)}$	8.17 ± 0.17
$[Cu_2L_2(OH)_2(H_2O)_2]^{6+} = [Cu_2L_2(OH)_3(H_2O)]^{5+} + H^+$	$pK_{a1(M_2L_2)}$	9.81 ± 0.02
$[Cu_2L_2(OH)_3(H_2O)]^{5+} = [Cu_2L_2(OH)_4]^{4+} + H^+$	$pK_{a2(M_2L_2)}$	10.45 ± 0.02

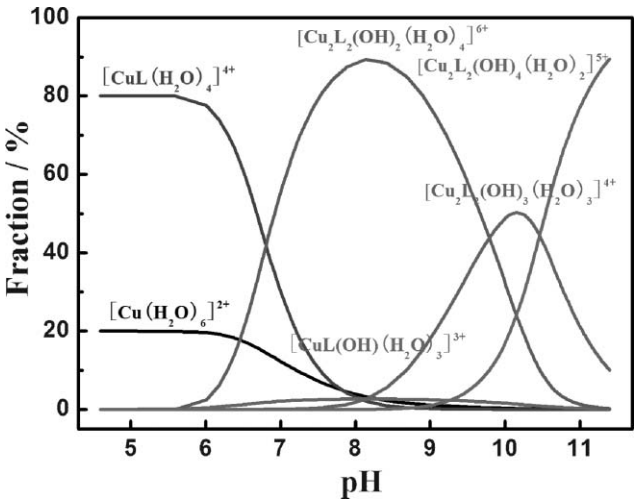

Fig. 2 Distribution plots of species with L^1 as a function of pH at 0.1 M $NaClO_4$ and 25 ± 0.1 °C.

In the case of the L^1, it is shown in Fig. 2 that five Cu(II) species are involved in complex formation at pH 5–11.5. Two simple mononuclear species, CuL^{4+} and $CuLH_{-1}^{3+}$ (charges of the ligand and coordinated water molecules are omitted for clarity), correspond to $[CuL(H_2O)_2]^{4+}$ and $[CuL(OH)(H_2O)]^{3+}$, respectively. Their equilibrium constants are shown in Table 1. Since guanidinium remains protonated over a wide pH range (pK_a = 12.5),[32] it is reasonable to assume that $Cu_2L_2H_{-2}^{6+}$, $Cu_2L_2H_{-3}^{5+}$ and $Cu_2L_2H_{-4}^{4+}$, are involved in the formation of μ-dihydroxo-structure dimer species, corresponding to $[Cu_2L_2(OH)_2(H_2O)_2]^{6+}$, $[Cu_2L_2(OH)_3(H_2O)]^{5+}$ and $[Cu_2L_2(OH)_4]^{4+}$, respectively. A possible μ-dihydroxo $Cu_2L_2H_{-2}^{6+}$ dimer has been isolated at pH ~12 and confirmed by elemental analysis (calc. (%) for: $(L^1H_{-2})_2Cu_2(\mu\text{-}OH)_2Cl_2(C_2H_5OH)\cdot 2H_2O$ (910.81): C 39.46, H 5.74, N 24.56, Found: C 39.56, H 5.31, N 24.61). The result also shows that

Table 2 Interaction of complexes with CT-DNA[a]

Complex	r^b	$\Delta T_m{}^c$/°C
1	0.1	4.24
	0.2	9.37
2	0.1	1.93
	0.2	3.26
3	0.1	0.72
	0.2	1.25

[a] *Reaction conditions*: 20 mM HEPES at pH 8.0, $I = 0.1$ M, [DNA] = 100 μM. [b] r = Molar ratio of complex/nucleic acid phosphate. [c] ΔT_m/°C = Melting temperature of DNA with complex minus the melting temperature of DNA alone.

guanidinium group always remains protonated in range of the measured pH.

In the presence of L^2, the titration of Cu(II) species were limited by precipitation of Cu(II) hydroxide at pH ≥ 7. This interfered with the saturation portion of the binding isotherm, making the curve fitting process impossible, so the data was not uploaded.

DNA affinity

The interaction between the two Cu(II) complexes **1** and **2** and the analogous non-pendant [Cu(bipy)Cl_2] (**3**) with calf thymus (CT) DNA is characterized by measuring their varying effects on the melting temperature of DNA (Table 2). The T_m curves were shown as Fig. S3 (ESI†). Considerable increase in the melting temperature in each case is observed, indicative of stabilization of the double-stranded nucleic acids by the metal complexes. A markedly larger stabilization effect of complex **1** over **2** is observed (Table 2). In general, there are at least three interaction modes between metal complexes and DNA: electrostatic interaction, hydrophobic binding and intercalating. Both complexes with dicationic pendants show higher affinity towards CT DNA than their analogue without any pendants, which suggests that the guanidinium/ammonium groups in **1** and **2** can be bound to the oxygen atoms of phosphate backbone.

Furthermore, the ΔT_m values of **1** are similar to those of the Cu(II) complex with tetraalkylammonium pendants reported by us,[30a] but their charge numbers are different ($[Cu(L^1)Cl_2]^{2+}$ and $[Cu(L)_2\ Br]^{5+}$, L = 5, 5′-di[1-(triethylammonio)methyl)-2,2′-dipyridyl). The X-ray structure analysis shows that, similarly to **1**, only two dicationic pendants of the $[Cu(L)_2Br]^{5+}$ ion can interact with the DNA backbone together with Cu(II) ion although it has four pendants in all. In the process of metal complex–DNA interaction, therefore, appended pendants are more influential than the ion charge.

DNA cleavage

Supercoiled plasmid DNA cleavage by the Cu(II) complexes and their analogues was studied in the absence of H_2O_2 or any reducing agents (Fig. 3) and a time-dependent cleavage was observed. We found that the supercoiled DNA (form I) was completely cleaved by **1** or **2** only after 2 h, but can not be completely cleaved by **3** even after 24 h. The cleavage activity of **1** is equivalent to **2**, and much higher than **3**.

In order to clarify the DNA cleavage mechanism, complexes **1** and **2** were investigated in the presence of chelating agent

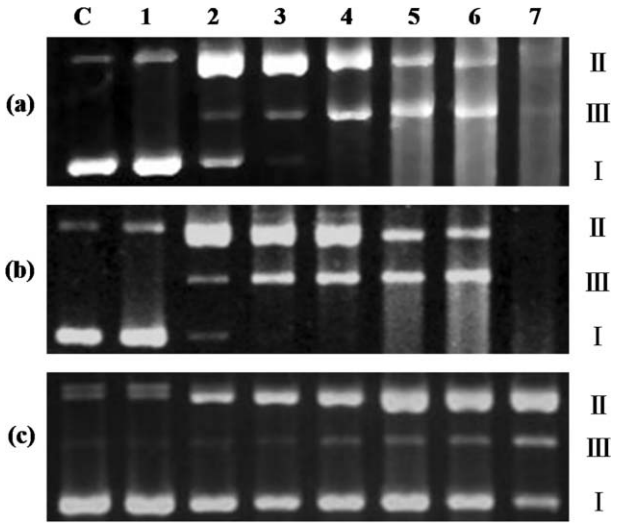

Fig. 3 Agarose gel electrophoresis of 38 μM bp pBR322 plasmid DNA at 37 °C in 20 mM HEPES at pH 7.2 in the presence of 150 μM **1** (a), **2** (b) and **3** (c). Lane 1: DNA control, lanes 2–8: DNA + complex for 0, 1, 2, 4, 8, 16, 24 h.

(EDTA) and hydroxyl radical scavengers (DMSO and *t*-BuOH).[33] As shown in Fig. 4, EDTA can efficiently inhibit the complex activity, however, both DMSO and *t*BuOH have no effect. This result can rule out the possibility of DNA cleavage by hydroxyl radicals. The cleavage was investigated further in the presence of catalase, which can lower solution concentrations of H_2O_2 (Fig. S6, ESI†). The negative result indicates that catalase does not inhibit DNA cleavage and so the mechanism of cleavage is not oxidative arising from $O_2^{\bullet -}$ and H_2O_2. In the absence of any reducing agents, therefore, DNA cleavage by **1** and **2** is likely to proceed *via* a hydrolytic degradative pathway.

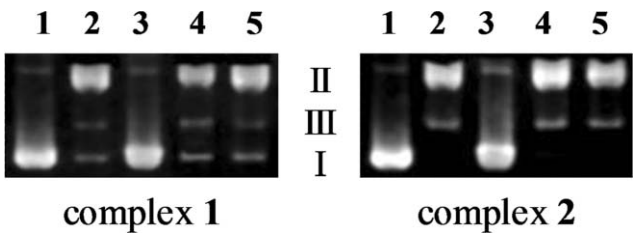

Fig. 4 Agarose gel showing cleavage of 38 μM bp pBR322 DNA incubated with complex (150 μM) in 20 mM HEPES, pH 7.2 at 37 °C for 1 h. Lane 1: DNA control, lane 2: DNA + complex, lanes 3–6: 0.1 M EDTA, DNA + complex + 1 M DMSO, 1 M tBuOH.

Direct evidence of DNA hydrolysis was obtained further from ligation experiments of pBR322 DNA linearized by **1**. It is well known that in DNA hydrolytic cleavage 3′-OH and 5′-OPO_3 (5′-OH and 3′-OPO_3) fragments remain intact and that these fragments can be enzymatically ligated and end-labeled.[34] We tried to recover the linear DNA from an agarose low melting point gel by cutting off the gel fragment and subjecting it to the DNA recovery system. The recovered linear DNA was subjected to overnight ligation reaction with T4 DNA ligase. The result after electrophoresis (Fig. 5) shows that the linear DNA fragments cleaved by **1** can be religated by T4 ligase just like linear DNA mediated by EcoRI. Hence, this result indicates that the process

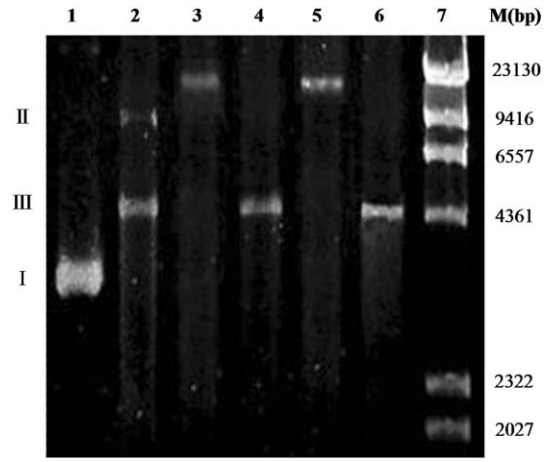

Fig. 5 Agarose gel electrophoresis for ligation of pBR322 DNA linearized by **1**: lane 1: DNA control, lane 2: DNA + 150 μM **1**; lanes 3 and 4: pBR322 DNA linearized by **1** with and without T4 DNA ligase; lanes 5 and 6: pBR322 DNA linearized by EcoRI with and without T4 DNA ligase; lane 7: λHindIII DNA markers.

of DNA cleavage by **1** is a hydrolysis that takes place by a reaction similar to that of the natural enzyme EcoRI.

Pseudo-Michaelis–Menten kinetics of DNA cleavage

All the complexes were tested for DNA cleavage under hydrolytic conditions, and a concentration-dependent cleavage was observed. Reaction that leads to formation of open circular DNA (form II) from the supercoiled from I over various concentrations of complexes **1**/**2** (60–300 μM) and **3** (150–1000 μM) and constant DNA concentration (38 μM, bp) was followed for different times at 37 °C (Fig. S4, ESI†). It is not an easy task to control the reaction conditions, and extract good quality rate data from gels. However, the disappearance of form I with time followed pseudo-first-order kinetic profiles and can be well fitted with a single-exponential decay curve. The k_{obs} for different concentrations and the degree for data fitting (R^2) are listed in Table S1, ESI.† Based on the plots of k_{obs} *vs.* concentrations of complex, saturation kinetics of DNA cleavage were observed at high concentration of complexes. The pseudo Michaelis–Menten kinetic parameters (k_{cat} and K_M) were calculated to be 4.42 ± 0.18 h^{-1} ($R^2 = 0.985$) and 7.46 × 10^{-5} M for **1**, 4.21 ± 0.11 h^{-1} ($R^2 = 0.968$) and 1.07 × 10^{-4} M for **2**, and 0.49 ± 0.13 h^{-1} ($R^2 = 0.953$) and 3.5 × 10^{-4} M for **3**, respectively, Fig. 6 and Fig. S7.

The obtained hydrolysis rate constants show that **1** and **2** have very high nuclease activities, giving *ca* 1.2 × 10^8-fold rate enhancement over the noncatalyzed hydrolysis of double-strand DNA. These values are also almost the same as for copper complexes with tetraalkylammonium pendants although dominant modes of their interactions with DNA are electrostatic interaction and hydrogen-bonding, respectively.[30] Likewise, the DNA cleavage activities of **1** and **2** are also about 10-fold higher than its simple analogue, **3**. Interestingly, under the same experimental condition of 20 mM HEPES, pH 7.2 at 37 °C for 1 h, DNA cleavage was not promoted distinctly by either free Cu^{2+}(aq) or free $L^{1/2}$ alone (Fig. S5, ESI†), which confirms that two electropositive pendants in **1** and **2** facilitate binding of the Cu(II)–bipy moiety to DNA and subsequently accelerates DNA cleavage. Rate constants of

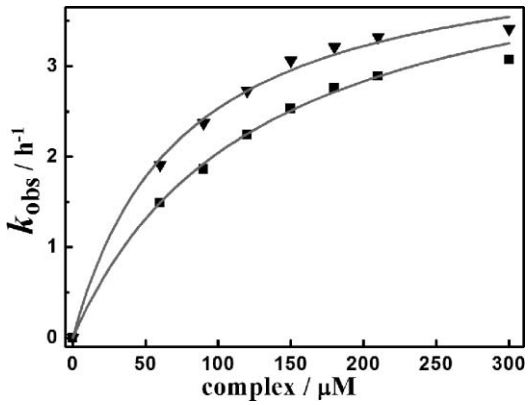

Fig. 6 Kinetics for the cleavage of plasmid pBR322 DNA by **1** (▼) and **2** (■) (60–300 μM) in 20 mM HEPES, pH 7.2 at 37 °C. The samples were run on a 0.9% agarose gel and stained with ethidium bromide.

DNA cleavage hydrolyzed by some Cu(II) complexes have been reported.[12,35–37] The rates are generally in the range of 10^{-2}–1.0 h^{-1}.[12] To our knowledge, few mononuclear complexes exhibited very high nuclease activities: examples include Cu–dpq (dpp = dipyrido[3,2-*d*:2′,3′-*f*]quinoxaline) with a rate constant of 5.58 h^{-1} at pH = 7.2,[35a] Cu–tach (tach = *cis*,*cis*-1,3,5-triaminocyclohexane) with a rate constant of 4.34 h^{-1} at pH = 8.1[36] and a Cu–neamin complex with the rate constant of 3.57 h^{-1} at pH = 7.3.[12]

The DNA cleavage by **1** under different pH values was investigated. The observed pH profile can be described by a bell-shaped curve with the maximum centered at pH ≈ 8 (Fig. 7(B)). It has been widely accepted that metal-bound hydroxyl species (LM–OH) are the active species in the hydration of the phosphate backbone.[1–11] As in previous research,[6,38] the formation of the active species from the precursor generally involves the steps of rapid exchange between coordinated halide and water molecules, followed by hydrolysis of the resulting aqua compounds to form a coordinated hydroxyl group that acts as a nucleophile for DNA cleavage. In solution, hydroxide complexes co-exist in comparable concentrations: mononuclear $Cu(L^1)(OH)$ and binuclear and $Cu_2(L^1)_2(OH)_2$, $Cu_2(L^1)_2(OH)_3$ and $Cu_2(L^1)_2(OH)_4$ species (Fig. 2).[38,39] As one can see from the results shown in Fig. 7, the pH-profiles of the observed fraction of DNA II and III cleaved by **1** superimposed with the distribution curve for the mononuclear hydroxide complexes is not consistent with the curve of the sum of mononuclear and binuclear hydroxide complexes. As shown in Fig. 7(B), the DNA cleavage rate V_{obs} and the pH dependencies of the concentration of $Cu(L^1)(OH)$ species were in agreement, indicating that the $Cu(L^1)(OH)$ species may be considered as a reactive form of the catalyst. However, the maximum attainable degree of formation of this species is only 2.8%, as is seen from the results in Fig. 7(B). It is worth noting that even with the active complex present at such a low amount one observes an unusually high k_{cat} value of 4.42 h^{-1} at physiological pH. This result can explain why DNA cleavage is very low when the total concentration of **1** is lower than 50 μM (due to too low active species concentration).

In view of the X-ray structure of **1** and the distance between adjacent phosphorus atoms of the phosphodiester in a DNA backbone, we suggest a mechanism which is similar to that proposed for $[Cu[9]aneCl_2]$ hydrolyzing phosphate diesters[38a] (Scheme 2). X-Ray analysis has confirmed that the distances between coordinated

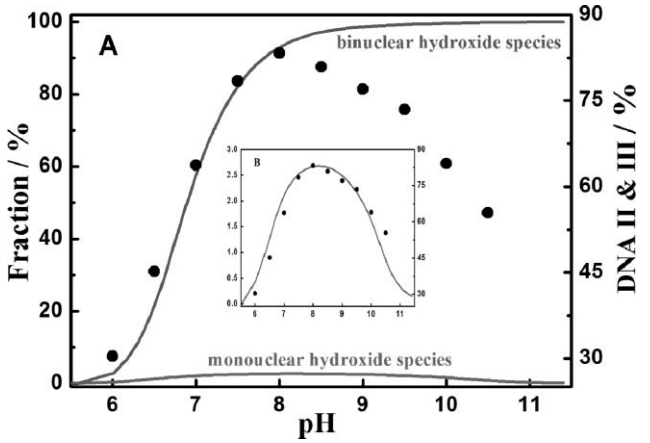

Fig. 7 Speciation diagram of Cu(II)–L^1 (left *y* axes) and pH dependence of DNA cleavage rate by **1** (●, right *y* axes). For (A), the dashed line represents the sum of $[CuL(OH)(H_2O)]^{3+}$ and $[Cu_2(\mu_2\text{-}OH)_2]^{2+}$ species $(Cu_2(L^1)_2(OH)_2$, $Cu_2(L^1)_2(OH)_3$ and $Cu_2(L^1)_2(OH)_4$ (coordinated water molecules and charges omitted)), the solid line corresponds to $[CuL(OH)(H_2O)]^{3+}$. (B) is the enlarged speciation diagram of $[CuL(OH)(H_2O)]^{3+}$ (left *y* axes) and pH dependence of DNA cleavage rate by **1** (●, right *y* axes). *Titration conditions*: $[L^1] = 1$ mM, [Cu(II)] = 1 mM, 0.1 M $NaClO_4$, 25 ± 0.1 °C. *Reaction conditions* for DNA cleavage: [DNA] = 38.0 μM bp, [**1**] = 150 μM, pH 6.0 (20 mM MES buffer), pH 6.5–7.0 (20 mM MOPSO buffer), pH 7.5–8.5 (20 mM Tris buffer), pH 9.0–9.5 (20 mM CHES buffer), pH 9.5–10.5 (20 mM CAPS buffer), 0.1 M $NaClO_4$, 37 ± 0.1 °C.

hydroxyl anion and quaternary guanidyl ion are around 6.5 Å in **1**, similar to the distance between adjacent phosphorus atoms of the phosphodiester in a DNA backbone (*ca.* 6 Å).[30] This suggests that the two guanidinium groups in **1** can synchronously interact with alternate phosphodiester groups in a DNA strand, Scheme 2(A). The direct interaction between the neighboring phosphoryl oxygen atoms and guanidinium groups facilitates the formation of an intermediate, which allows the DNA to be cleaved readily. Therefore, the higher activity of **1** can be attributed to its structure matching with the phosphodiester backbone of nucleic acid and cooperative interaction from the highly active bipy–Cu(II) moiety and two positive guanidinium groups.

Conclusion

Two new Cu(II) complexes are formed and isolated when copper(II) is reacted with any molar ratio of 5,5′-dimethyl-2,2′-bipyridyl derivatives with guanidinium/ammonium pendants. The complexes with guanidinium/ammonium pendants exhibit very high DNA affinity and nuclease activity. For the complex with guanidinium pendants, the observed reactivity is entirely due to the mononuclear hydroxide species and give 10-fold rate acceleration for hydrolyzing the phosphate diesters than their unmodified analogue even though its concentration in aqueous solution is less than 3% due to strong dimerization. The enhanced acceleration could be attributed to electrostatic interaction between the positive pendants with guanidinium/ammonium groups of the complexes and the phosphodiester backbone of nucleic acid.

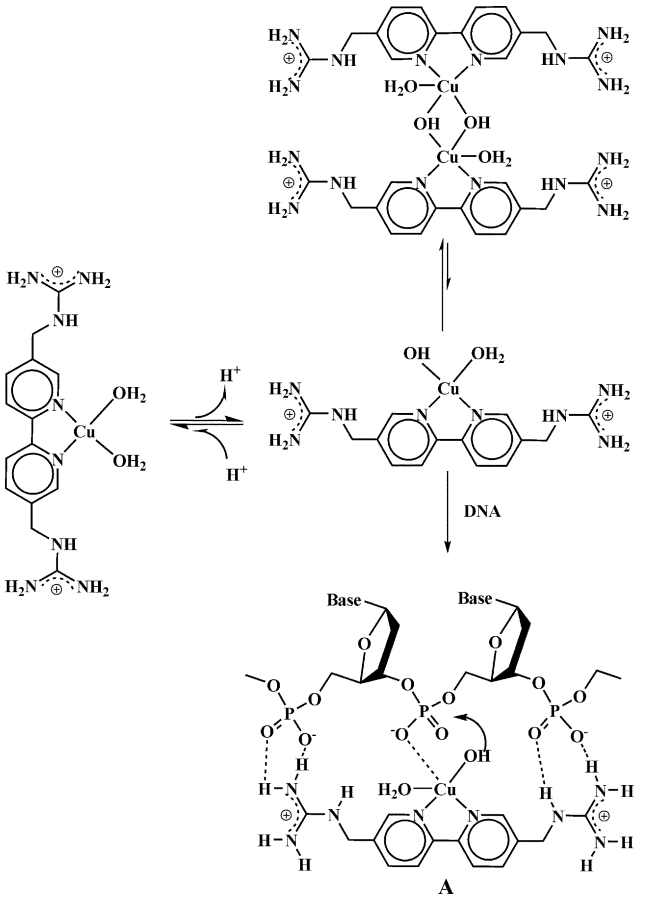

Scheme 2 Proposed mechanism for the DNA cleavage by **1**.

Experimental

Materials

5,5′-Dimethyl-2,2′-dipyridyl was purchased from Aldrich Chemical Co. The pBR322 DNA was purchased from MBI. Catalase was purchased from BBI. Ethidium bromide and HEPES were purchased from AMRESCO. T4 DNA ligase and EcoRI enzyme was purchased from Toyobo Co., Ltd. Other reagents of analytical grade were obtained from commercial suppliers and used directly without further purification. Milli-Q water was used in all physical measurement experiments.

Preparation of ligands

The ligands were synthesized according to Scheme 3, while the derivatives of 5,5′-dimethyl-2,2′-dipyridyl (**b**, **c**) were synthesized as in the previous method.[31a]

5,5′-Di[1-(guanidyl)methyl]-2,2′-bipyridyl chloride (L^1·2Cl). 1*H*-Pyrazole-1-carboxamidine monohydrochloride (1.47 g, 10 mmol) and *N*,*N*-diisopropylethylamine (3.5 mL, 20.0 mmol) were dissolved in dry DMF (10 mL), stirred under N_2 for 10 min, then L^2 (1.07 g, 5 mmol) was added into the mixture. The mixture solution was stirred for 30 h under N_2 at room temperature. 50 mL acetone was added dropwise into the mixture and the resulting precipitate was filtered off and washed with ethanol to give a straw yellow powder (1.3 g, 70%). ESI-MS:

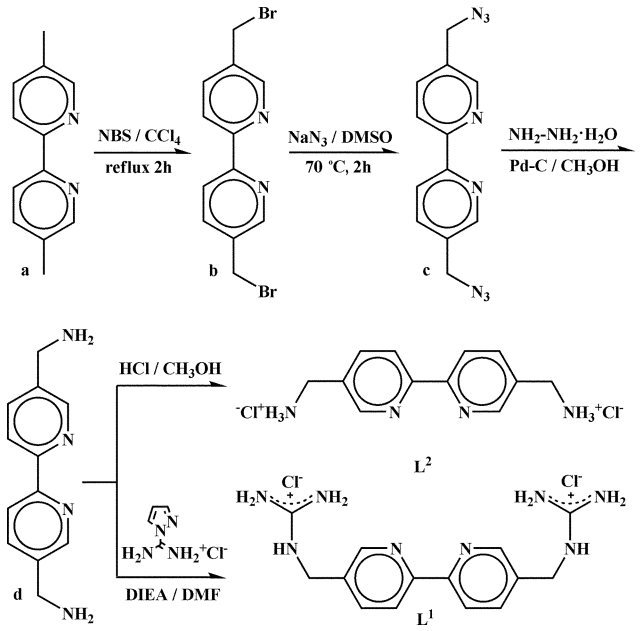

Scheme 3 Schematic view of the synthetic route for the ligands.

299 [M + H]$^+$, 150 [M + 2H]$^{2+}$/2. Elemental analysis: calc. (%) for ($C_{14}H_{20}N_8Cl_2$·0.3CH_3OH (380.89): C 45.07, H 5.63, N 29.34; found: C 45.55, H 5.56, N 28.92. ^{1}H NMR (DMSO, 300 MHz): δ 8.623 (s, 2 H, PyH), 8.386 (d, 2 H, PyH), 7.871 (d, 2 H, PyH), 4.503 (d, 4 H, $NHCH_2$ Py).

5,5′-Di[1-(amino)methyl]-2,2′-bipyridyl chloride (L^2·2Cl). L^2·2Cl was synthesized according to literature.[40]

Preparation of copper complexes

CAUTION: Although no problems were encountered in this work, transition-metal perchlorates are potentially explosive and should thus be prepared in small quantities and handled with care.

[Cu(L^1)Cl_2](ClO_4)$_2$·H_2O (1). A methanol solution of $Cu(ClO_4)_2$·$6H_2O$ (60 mg, 0.16 mmol) was added dropwise into a solution of L^2·2Cl (50 mg, 0.135 mmol) in 10 mL of water and a green solution was obtained after stirring for 4 h. The solution was filtered and allowed to stand for evaporation. Several days later, green crystals suitable for X-ray analysis were obtained. Elemental analysis data: calc. (%) for $Cu(C_{14}H_{20}N_8)Cl_2(ClO_4)_2$·$H_2O$ (651.73): C 25.80, H 3.40, N 17.19; found: C 26.22, H 3.14, N 17.07.

[Cu(L^2)Cl_2](ClO_4)$_2$ (2). Complex **2** was prepared in the same way as above. Elemental analysis data: calc. (%) for $Cu(C_{12}H_{16}N_4)Cl_2(ClO_4)_2$ (549.64): C 26.22, H 2.93, N 10.19; found: C 26.70, H 3.19, N 9.85.

General methods

Microanalyses (C, H and N) were carried out with an Elementar Vario EL elemental analyser. UV-vis spectroscopy was recorded on a Varian Cary 100 spectrophotometer with a thermostatic cell holder and NMR spectroscopy was performed on a Varian Inova 500/Mercury plus 300 NMR spectrometer with D_2O or DMSO-d_6 as solvent. An LCQ DECA XP electrospray mass spectrometer was employed for the investigation of charged ligands in a mixture of water and methanol.

Table 3 Crystallographic data for **1**

Complex	**1**
Empirical formula	$C_{14}H_{20}Cl_4CuN_8O_8$
M_r	633.72
T/K	293(2)
λ/Å	0.71073
Crystal system	Monoclinic
Space group	$C2/c$
a/Å	17.202(3)
b/Å	8.9681(13)
c/Å	15.145(2)
β/°	92.609(3)
V/Å^3	2334.0(6)
Z	4
D_c/g cm^{-3}	1.803
μ/mm^{-1}	1.454
F(000)	1284
Crystal size/mm	0.325 × 0.324 × 0.206
θ range for data collection/°	2.56–27.00
Limiting indices, hkl	−12 to 21, −7 to 11, −19 to 19
Reflections collected	4360
Independent reflections (R_{int})	2419 (0.0217)
Goodness-of-fit on F^2	1.019
R/wR_2 [$I > 2\sigma(I)$]	0.0508/0.1301
R/wR_2 (all data)[a]	0.0624/0.1380
$\Delta\rho_{max,min}$/e Å^{-3}	0.685/−0.315

[a] $R_1 = \sum||F_o| - |F_c||/\sum|F_o|$, $wR_2 = [\sum w(F_o^2 - F_c^2)^2/\sum w(F_o^2)^2]^{1/2}$.

X-Ray crystallography

Single-crystal X-ray data of **1** was collected on a Bruker Smart Apex CCD diffractometer at 293 K with graphite-monochromated Mo-Kα radiation (λ = 0.71073 Å). The reflections were corrected for Lorentz and polarization effects and empirical absorption corrections were applied using the SADABS program. The space groups were determined from systematic absences and confirmed by the results of refinement. The structures were solved by direct methods using the SHELXTL software and all non-H atoms were refined with anisotropic displacement parameters.[41] The crystallographic data are given in Table 3.

CCDC reference number 632380.

For crystallographic data in CIF or other electronic format see DOI: 10.1039/b801549j

Potentiometric titration

An automatic titrator (Metrohm 702 Titrino) coupled to a Metrohm electrode was used and calibrated according to the Gran method.[42,43] The electrode system was calibrated with buffers and checked by titration of $HClO_4$ with 0.10 M NaOH. All titrations were carried out under a N_2 flow to eliminate the presence of atmospheric CO_2, at 25.0 ± 0.1 °C and 0.10 M $NaClO_4$. The measurements were carried out in a thermostated cell containing a complex solution (25 mmol/25 mL) with ionic strength of 0.10 M $NaClO_4$. The sample was titrated by addition of fixed volumes of a standard CO_2-free NaOH solution (0.10 M). Duplicate measurements were performed, for which the experimental error was below 1%. The titration data were fitted with the HYPERQUAD program[44] to calculate the ligand protonation constants

K_n, the complex-formation constant, K_{ML}, and the deprotonation constants of the coordinated water molecules.

Thermal melting curves and ΔT_m calculation

The concentration of the calf thymus (CT) DNA was determined spectrophotometrically on the basis of known molar extinction coefficient (ε_{260}) 6600 $dm^3\ mol^{-1}\ cm^{-1}$.[30,45] Thermal melting curves were obtained on a Cary 100 UV-vis spectrophotometer connected to a temperature controller. The melting curves were recorded at different molar ratios of compound to DNA (r) by measurement of the changes in absorption at 260 nm as function of temperature in the range of 55–95 °C. T_m values were determined from the maximum of the first derivative or tangentially from the graph at the midpoint of the transition curves. ΔT_m values were calculated by subtracting T_m of the free nucleic acid from the T_m of the nucleic acid interacted with the complex.

DNA cleavage and k_{obs} calculation

The rates of DNA cleavage at various catalyst concentrations were determined in 20 mM HEPES, pH 7.2, at 37 °C for different intervals of time according to our previous report.[30] After incubation of the pBR322 DNA and complex for a defined time, 4 μL of loading buffer (bromophenol blue, 50% glycerol, and 2 mM EDTA) was added and stored at −20 °C. The samples were then loaded directly onto a 0.9% agarose gel and electrophoresed at a constant voltage of 70 mV for 120 min. The gels were visualized in an electrophoresis documentation and analysis system 120. Densitometric calculations were made using the analysis method in Image Tools 3.00. The intensities of supercoiled pBR322 DNA were corrected by a factor of 1.42 as a result of its lower staining capacity by ethidium bromide. The decrease of form I was fitted to a single exponential decay curve (pseudo-first-order kinetics) by use of eqn 1(a) or (b), where y_0 is the initial percentage of a form of DNA, y is the percentage of a specific form of DNA at time t, a is the percentage of uncleaved DNA, and k_{obs} is the hydrolysis rate, or apparent rate constant.

$$y = (y_0 - a)\exp(-k_{obs}x) + a \quad (1a)$$

$$y = (100 - y_0)(1 - \exp(-k_{obs}x)) \quad (1b)$$

Further, saturation kinetic of DNA cleavage was studied using various complex concentrations. Based on the plots of k_{obs} *vs.* concentrations of complex, the pseudo-Michaelis–Menten kinetic parameters were calculated.

DNA ligation

After incubation of pBR322 DNA with 150 μM **1** and EcoRI for 16 h at 37 °C respectively, the cleavage product, *i.e.* linear form, was purified by a DNA Gel Extraction Kit. The ligation reaction of the linearized plasmid was performed as follows:[46,47] a mixture of 1 μL T4 ligase (4 units) and 1 μL 10 × ligation buffer containing 1 mM ATP, 5 μL of the solution containing DNA cleavage fragment linearized by **1** and 3 μL H_2O, 2 μL of the solution containing DNA cleavage fragment linearized by EcoRI and 6 μL H_2O, were incubated for 20 h at 16 °C. Afterwards, the ligation products were electrophoresed, stained and imaged. The remaining solution containing DNA cleavage fragment was kept at −20 °C.

Acknowledgements

This work was supported by the National Natural Science Foundation of China (20725103, 30770494, 20671098, 20529101), the Guangdong Provincial Natural Science Foundation (07117637) and National Basic Research Program of China (973 Program).

Notes and references

1 Q. Jiang, N. Xiao, P. F. Shi, Y. G. Zhu and Z. J. Guo, *Coord. Chem. Rev.*, 2007, **251**, 1951.
2 F. Mancin, P. Scrimin, P. Tecillab and U. Tonellato, *Chem. Commun.*, 2005, 2540.
3 J. Suh, *Acc. Chem. Res.*, 2003, **36**, 562.
4 (*a*) A. Sreedhara and J. A. Cowan, *J. Biol. Inorg. Chem. Acc. Chem. Res.*, 2001, **6**, 337; (*b*) J. A. Cowan, *Chem. Rev.*, 1998, **98**, 1067.
5 N. H. Williams, B. Takasaki, M. Wall and J. Chin, *Acc. Chem. Res.*, 1999, **32**, 485.
6 E. L. Hegg and J. N. Burstyn, *Coord. Chem. Rev.*, 1998, **173**, 133.
7 C. J. Burrows and J. G. Muller, *Chem. Rev.*, 1998, **98**, 1109.
8 W. K. Pogozelski and T. D. Tullius, *Chem. Rev.*, 1998, **98**, 1089.
9 R. R. Breaker, *Chem. Rev.*, 1997, **97**, 371.
10 D. E. Wilcox, *Chem. Rev.*, 1996, **96**, 2435.
11 D. S. Sigman, A. Mazumder and D. M. Perrin, *Chem. Rev.*, 1993, **93**, 2295.
12 A. Sreedhara, J. D. Freed and J. A. Cowan, *J. Am. Chem. Soc.*, 2000, **122**, 8814.
13 E. Kovari, J. Heitker and R. Kramer, *J. Chem. Soc., Chem. Commun.*, 1995, 1205.
14 R. Hettich and H. J. Schneider, *J. Am. Chem. Soc.*, 1997, **119**, 5638.
15 R. H. Terbrueggen, T. W. Johann and J. K. Barton, *Inorg. Chem.*, 1998, **37**, 6874.
16 S. Aoki, K. Iwaida, N. Hanamoto, M. Shiro and E. Kimura, *J. Am. Chem. Soc.*, 2002, **124**, 5256.
17 J. F. Folmer-Andersen, H. Ait-Haddou, V. M. Lynch and E. V. Anslyn, *Inorg. Chem.*, 2003, **42**, 8674.
18 C. Schmuck, *Coord. Chem. Rev.*, 2006, **250**, 3053.
19 C. Schmuck and U. Machon, *Chem.–Eur. J.*, 2005, **11**, 1109.
20 M. D. Best, S. L. Tobey and E. V. Anslyn, *Coord. Chem. Rev.*, 2003, **240**, 3.
21 D. M. Perreault, L. A. Cabell and E. V. Anslyn, *Bioorg. Med. Chem.*, 1997, **5**, 1209.
22 S. L. Tobey and E. V. Anslyn, *J. Am. Chem. Soc.*, 2003, **125**, 14807.
23 R. J. T. Houk, S. L. Tobey and E. V. Anslyn, *Top. Curr. Chem.*, 2005, **255**, 199.
24 K. A. Schug and W. Lindner, *Chem. Rev.*, 2005, **105**, 67.
25 F. P. Schmidtchen and M. Berger, *Chem. Rev.*, 1997, **97**, 1609.
26 C. Bailly, R. K. Arafa, F. A. Tanious, W. Laine, C. Tardy, A. Lansiaux, P. Colson, D. W. Boykin and W. D. Wilson, *Biochemistry*, 2005, **44**, 1941.
27 N. Strater, T. Klabunde, P. Tucker, H. Witzel and B. Krebs, *Science*, 1995, **268**, 1489.
28 J. P. Griffith, J. L. Kim, E. E. Kim, M. D. Sintchak, J. A. Thomson, M. J. Fitzgibbon, M. A. Fleming, P. R. Caron, K. Hsiao and M. A. Navia, *Cell*, 1995, **82**, 507.
29 M. Terada, H. Ube and Y. Yaguchi, *J. Am. Chem. Soc.*, 2006, **128**, 1454.
30 (*a*) X. Chen, J. Wang, S. Sun, J. Fan, S. Wu, J. Liu, S. Ma, L. Zhang and X. Peng, *Bioorg. Med. Chem. Lett.*, 2008, **18**, 109; (*b*) X. Sheng, X. M. Lu, J. J. Zhang, Y. T. Chen, G. Y. Lu, Y. Shao, F. Liu and Q. Xu, *J. Org. Chem.*, 2007, **72**, 1799; (*c*) S. J. Franklin and J. K. Barton, *Biochemistry*, 1998, **37**, 16093; (*d*) R. H. Terbrueggen, T. W. Johann and J. K. Barton, *Inorg. Chem.*, 1998, **37**, 6874.
31 (*a*) Y. An, M. L. Tong, L. N. Ji and Z. W. Mao, *Dalton Trans.*, 2006, 2066; (*b*) Y. An, Y. Y. Lin, H. Wang, H. Z. Sun, M. L. Tong, L. N. Ji and Z. W. Mao, *Dalton Trans.*, 2007, 1250.
32 A. Gobbi and G. Frenking, *J. Am. Chem. Soc.*, 1993, **115**, 2362.
33 O. I. Aruoma, B. Halliwell and M. Dizdaroglu, *J. Biol. Chem.*, 1989, **264**, 13024.

34 (*a*) M. E. Branum, A. K. Tipton, S. Zhu and L. Que, Jr., *J. Am. Chem. Soc.*, 2001, **123**, 1898; (*b*) B. Weiss, A. Jacquemin-Sablon, T. R. Live, G. C. Fareed and C. C. Richardson, *J. Biol. Chem.*, 1968, **243**, 4543.
35 S. Dhar, P. A. N. Reddy and A. R. Chakravarty, *Dalton Trans.*, 2004, 697.
36 T. Itoh, H. Hisada, T. Sumiya, M. Hosono, Y. Usui and Y. Fujii, *Chem. Commun.*, 1997, 677.
37 E. L. Hegg and J. N. Burstyn, *Inorg. Chem.*, 1996, **35**, 7474.
38 (*a*) K. A. Deal and J. N. Burstyn, *Inorg. Chem.*, 1996, **35**, 2792; (*b*) E. L. Hegg, S. H. Mortimore, C. L. Cheung, J. E. Huyett, D. R. Powell and J. N. Burstyn, *Inorg. Chem.*, 1999, **38**, 2961; (*c*) M. Scarpellini and A. Neves, *Inorg. Chem.*, 2003, **42**, 8353; (*d*) M. J. Belousoff, M. B. Duriska, B. Graham, S. R. Batten, B. Moubaraki and K. S. Murray, *Inorg. Chem.*, 2006, **45**, 3746.
39 T. Kobayashi, S. Tobita, M. Kobayashi, T. Imajyo, M. Chikira, M. Yashiro and Y. Fujii, *J. Inorg. Biochem.*, 2007, **101**, 348.
40 L. Jicsinszky and R. Iványi, *Carbohydr. Polym.*, 2001, **45**, 139.
41 G. M. Sheldrick, SHELXS-97 *Program for Crystal Structure Solution*, Goettingen University, Germany, 1997.
42 G. Gran, *Acta Chem. Scand.*, 1950, **4**, 559.
43 Z. W. Mao, G. Liehr and R. van Eldik, *J. Chem. Soc., Dalton Trans.*, 2001, 1593.
44 P. Gans, A. Sabatini and A. Vacca, *Talanta*, 1996, **43**, 1739.
45 D. K. Chand, H. J. Schneider, A. Bencini, A. Bianchi, C. Giorgi, S. Ciattini and B. Valtancoli, *Chem.–Eur. J.*, 2000, **6**, 4001.
46 L. M. T. Schnaith, R. S. Banson and L. Que, Jr., *Proc. Natl. Acad. Sci. U. S. A.*, 1994, **91**, 569.
47 C. Liu, S. Yu, D. Li, Z. Liao, X. Sun and H. Xu, *Inorg. Chem.*, 2002, **41**, 913.

